Journal of Biomaterials Science, Polymer Edition

ISSN: 0920-5063 (Print) 1568-5624 (Online) Journal homepage: https://www.tandfonline.com/loi/tbsp20

Biological properties of electrospun cellulose scaffolds from biomass

Debora Ferreira Laurito Friend, Maria Elena Leyva González, Mirta Mir Caraballo & Alvaro Antonio Alencar de Queiroz

To cite this article: Debora Ferreira Laurito Friend, Maria Elena Leyva González, Mirta Mir Caraballo & Alvaro Antonio Alencar de Queiroz (2019): Biological properties of electrospun cellulose scaffolds from biomass, Journal of Biomaterials Science, Polymer Edition, DOI: 10.1080/09205063.2019.1636351

To link to this article: https://doi.org/10.1080/09205063.2019.1636351

Accepted author version posted online: 24 Jun 2019.
Published online: 09 Jul 2019.

JOURNAL OF BIOMATERIALS SCIENCE, POLYMER EDITION
https://doi.org/10.1080/09205063.2019.1636351

Biological properties of electrospun cellulose scaffolds from biomass

Debora Ferreira Laurito Friend[a], Maria Elena Leyva González[b], Mirta Mir Caraballo[c] and Alvaro Antonio Alencar de Queiroz[d]

[a]Post Graduate Program in Materials for Engineering, Federal University of Itajubá (UNIFEI), Itajubá-MG, Brazil; [b]Physics and Chemistry Institute (IFQ), Federal University of Itajubá (UNIFEI), Itajubá-MG, Brazil; [c]Institute of Exact Sciences, ICEX - Federal University of Alfenas (Unifal-MG), Alfenas-MG, Brazil; [d]High Voltage Laboratory Prof. Manuel Luís Barreira Martinez (LAT-EFEI)/Institute of Electrical Systems and Energy (ISEE), Federal University of Itajubá-UNIFEI, Itajubá-MG, Brazil

ABSTRACT

Nowadays the development of sustainable technologies for the effective production of polymeric materials that can be used as biomaterials will be of importance. In this work, cellulose (CEL) was purified from potato peel waste (PPW) and used to produce electrospun nanofibers for tissue engineering applications. The purified CEL was solubilized in copper ethylenediamine (Cuen) and the electrospun nanofibers was produced through electrospinning technique in diameter range of 250–500 nm at electrical field strength of 20 kV. To confirm the applicability of the electrospun CEL scaffolds in tissue engineering, in vitro BALB-3T3 fibroblastic cell adhesion and cell proliferation tests were employed in this study. Cell viability was evaluated by staining with ethidium bromide (EtBr) and acridine orange (AO) to evaluate the possible effects of cytotoxicity of the CNF scaffolds. Fluorescence studies confirmed that BALB-3T3 viable cells attached and spread throughout the CEL scaffold. The attachment and spreading of viable cells suggests that electrospun CEL scaffolds support growth of BALB-3T3 fibroblasts cells and suggests that PPW can be a useful source of raw material for the production of scaffolds for tissue engineering.

ARTICLE HISTORY
Received 10 April 2019
Accepted 23 June 2019

KEYWORDS
Cellulose; electrospinning; scaffolds; BALB-3T3

1. Introduction

Nowadays, cellulosic biomass has gained a lot of attention as a useful source or raw material for the sustainable production of cellulose-based biomaterials [1–4]. In line with the current focus on the sustainable economy development and environmental concerns, the exploitation of the cellulosic biomass from agricultural wastes for biomedical applications represents a promising potential as an alternative to fossil resources [5,6]. Additionally, the use of agricultural wastes in the production of high

CONTACT Alvaro Antonio Alencar de Queiroz dealenquer@gmail.com alvaro.alencar@pq.cnpq.br High Voltage Laboratory Prof. Manuel Luís Barreira Martinez (LAT-EFEI)/Institute of Electrical Systems and Energy (ISEE), Federal University of Itajubá-UNIFEI, Itajubá-Minas Gerais, 37500-903, Brazil.

value added biopolymers for use in biomaterials industry may be considered to be an important step in the agrotechnology development [7–10].

Potatoes (*Solanum tuberosum subesp*), are one of the most abundant renewable source of cellulose that could be recovered and properly processed into materials suitable for the production of cellulose-based biomaterials [11]. The potatoes industries generate a large quantity of potato peel waste (PPW) which has been primarily used as local animal feed. However, PPW has a great potential for the production of cellulose nanofibers (CNF) which can be used for production of scaffolds for tissue engineering [12–16].

After a pretreatment step to isolate cellulose (CEL), the electrospinning technique can be used to produce scaffolds applicable to tissue engineering. This method requires a high voltage, which is able to accelerate a polymer solution through a metal capillary. Considering an intense electrical field, a solution jet reaches a grounded target (collector) that leads to solvent evaporation and consequently generation of nanofibers. The quality of the fibers produced, including diameter and morphology, relies on electrospinning variables, such as solution composition, applied voltage, collector distance, and collector type [17].

Since CEL is insoluble in most organic solvents, several studies have focused on the electrospinning not directly from cellulose but in its derivatives. In many of these studies cellulose acetate (CA), hydroxypropyl cellulose (HPC), hydroxypropylmethyl cellulose (HPMC) and ethyl-cyanoethyl cellulose (ECC) were used as the starting material and after electrospinning process were subsequently deacetylated by alkaline hydrolysis to produce a regenerated based-cellulose scaffold [18,19].

CNF have been intensely explored as biomaterial for tissue engineering scaffolds due to their mechanical properties and the ideal interconnected porosity for production of scaffolds for tissue engineering [20–25]. The several studies on the feasibility for CNF scaffolds as biomaterials for skins replacements for burnings and wounds, drugs releasing system, blood vessel growth, nerves, gum and dura-mater reconstruction, scaffolds for tissue engineering stent covering and bone reconstruction shows the greater potential of the agrotechnology sector for recovery CEL through the treatment of PPW [26–31].

In spite of the large number of investigations about the electrospinning of biocomposites based on CEL nanofillers and the CEL-derivatives from agricultural wastes [32], no studies were identified on the direct electrospinning of CEL from PPW and, as far as the authors are aware, the direct electrospinning of CEL from PPW without the alkaline regeneration step were reported till the moment. In particular, electrospinning of CEL derived from PPW has never been reported, probably because the focus on this material has been concentrated mainly on their uses for the production of animal feed, fertilizer and biosynthesis industries [33].

Considering the fact that PPW is renewable, abundant and low cost, this work presents the extraction, purification and electrospinning of CEL from PPW to obtain scaffolds for tissue engineering. CEL from PPW was characterized through attenuated total reflection Fourier transform infrared (ATR-FTIR), X-ray diffraction (XRD) and scanning electron microscopy (SEM) analyses. Copper ethylenediamine (Cuen) was used as ionic liquid for dissolution of CEL. The primary aim was achieved to develop

stable and pure scaffolds for biomedical applications. Furthermore, the surface morphology of the scaffolds were then analysed through SEM analysis and their viability on human fibroblasts was investigated for its suitability for tissue engineering applications.

2. Materials and methods

2.1. Materials

PPW was obtained from the local industry in south of Minas Gerais (Itajubá), Brazil, at world geodetic system-1984 (WGS-84) latitude of 22°25′22.7″S and longitude of 45°27′36.9″W, coordinates. The raw material was cut into pieces of approximately 3 cm length, washed thoroughly to remove dust and debris and then dried in oven for 36 hr at 70 °C. The dried potato peel was grind to fine powder using in a knife mill (Didática-SP) with a 20 mesh screen, to obtain a fine granulometry. The grinded sample was then homogenized and conditioned in low density polyethylene bags (Braskem) and stored in the refrigerator (4 °C) before use.

The analytical grade reagents such as sodium hydroxide (NaOH, 97% m/m), ethanol, hydrogen peroxide (H_2O_2, 35% v/v), lactic acid ($C_3H_6O_3$), glycidol ($C_3H_6O_2$) and copper ethylenediamine (Cuen) were obtained from Sigma-Aldrich and were used as received.

2.2. Isolation of cellulose from potato peel waste

PPW is mainly composed by starch, cellulose, hemicellulose and lignin, and therefore required an initial chemical treatment step including delignification and bleaching to isolate pure CEL [31]. In this work, 25.0 grams of dry mass ground of PPW was initially treated with a 0.5 N aqueous sodium hydroxide solution (NaOH) at 80 °C for 2.5 hours under constant stirring [33]. This delignification step was repeated twice to the completely elimination of starch, lignin and hemicellulose. After each treatment, the pulp was filtered and washed with deionized water to pH close to neutrality (7.0). A sieve of 200 mesh (75 μm ABNT) stainless steel sieve (Granute ST) was used to remove the dissolved impurities. The delignification step was followed by cellulose bleaching treatment with 2.3 wt% hydrogen peroxide at 70 °C for 2 hours under constant stirring. The purified cellulose (CEL) from PPW was thoroughly washed with deionized water to pH 7.0 and lyophilized (Freeze-dried model Supermodulyo with refrigerated chamber Edwards).

2.3. ECL nanofibers electrospinning

Purified CEL was dissolved in copper ethylenediamine (Cuen) at concentration of 10% w/w under magnetic stirring at room temperature (25 °C) until a clear solution was obtained (24 hr) [34]. Hyperbranched polyglycerol (HPGL, molecular weight of 1.5 kDa) was prepared in our laboratories by a one-step synthesis via ring-opening multi-branching polymerization of glycidol stitch [35]. HPGL was added to CEL-Cuen solution at concentration of 4 wt% to regulate the solution viscosity making the

CEL-Cuen solution electrospinnable. The CEL-Cuen solution was feed into 20 mL syringe equipped with a 20 gage needle (inner diameter of 0.58mm and 39 mm long). The flow rate of the solution through the needle was controlled to be on the order of 0.1 mL/min through an infusion pump (Lifemed LF 2001). A copper mesh (Tegape, 100 mm × 100 mm) with aluminum foil (Liondor, thickness of 0.050 mm) on top was used as the grounded collector being 10 cm far from the needle tip. A voltage of 10 kV supplied by a high voltage power supply (Phywe) was applied for a time of 3 min at room temperature (25 °C). The CNF deposited on the collection plate was weighed and stored in a desiccator under vacuum at room temperature (25 °C).

For the extraction of Cuen the CNF electrospun scaffolds were thoroughly washed in three steps with a solution of ammonium hydroxide (NH_4OH, 2% v/v) and rinsing with a solution of lactic acid at 5% w/w. The CNF scaffolds were air dried at 25 °C under vacuum desiccator (Laborglass).

2.4. Characterization methods

The purified CEL was characterized by attenuated total reflection Fourier transform infrared (ATR-FTIR) technique. ATR-FTIR spectroscopy was carried out on the CEL samples by means of a Perkin Elmer Spectrum 100 spectrometer, equipped with a Universal ATR diamond crystal sampling accessory. Infrared spectra were recorded by accumulating up to 32 scans with a resolution of 4 cm^{-1}, in the range of 4000–400 cm^{-1}.

X-ray diffraction (XRD) analyses were done in order to determine the crystallinity of extracted CEL from PPW. The XRD pattern was obtained using X-ray diffractometer (XRD- D2000 diffractometer, Rigaku) with filtered Cu Kα radiation operated at 40 kV and 40 mA. The XRD pattern was recorded from 5 to 50° (2 θ), with a scanning speed of 2°/min. The crystallinity index (IC) of extracted CEL was determined using the height of the CEL 002 peak (I_{002}, 2 $\theta = 22.5°$) and the minimum intensity between the 002 200 and 110 peaks (I_{am}, $2\theta = 22°$) expressed by [36]:

$$IC(\%) = \frac{I_{002} - I_{am}}{I_{002}} \times 100 \quad (1)$$

where I_{002} represent the height of the 002 peak ($2\theta = 22°$) associated with the crystalline region of CEL; I_{am} represent the amorphous regions in the cellulose and correspond to intensity of diffraction pattern at $2\theta = 22°$.

The morphological characterization of extracted CEL was performed using a scanning electron microscopy (SEM) Shimadzu Superscan SSX-550 SEM scanning electron microscope with an acceleration voltage of 4–10 kV. The samples were mounted onto stubs by means of carbon adhesive tape and coated with a 20 nm thick gold layer by means of a modular high vacuum coating system.

The diameters of the CNF scaffolds were analysed by the free software JImage from SEM images in according to methodology adapted from literature [37]. To evaluate the diameters of CNF, every SEM micrograph was divided into 3 regions horizontally and 4 regions vertically. The diameter of 60 CNF was measured in every SEM image.

2.5. Biological assays

2.5.1. Cell adhesion and cell growth assay

3T3 Fibroblasts (BALB/c clone A31, American Type Culture Collection CCL 173) were cultured in Dulbecco's modified Eagle's medium (DMEM, LGC, Biotecnologia Ltda), and supplemented with 10% fetal bovine serum (Laborclin, FBS), 1% (w/w) glutamine (Gibco) and 1% (w/w) gentamicin (Gibco), to form a subconfluent monolayer on the electrospun scaffolds. A 500 μL cell suspension containing 10,000 cells/cm^2 was added to the top of electrospun CNF scaffolds with and the aid of a stainless steel ring 316 NL of 1 cm in diameter, thus delimiting the area of application and grown to near confluency over 2–3 days at 37 °C and 95% humidity in 5% CO_2 atmosphere.

2.5.2. Morphological analysis

The BALB-3T3 cells in scaffold surfaces were fixed with 2% glutaraldehyde (Sigma-Aldrich) in 0.1 M phosphate-*buffered* saline (PBS, 8 g of NaCl; 0.2 g of KCl; 1.44 g of Na_2HPO_4; 0.24 g of KH_2PO_4, Sigma-Aldrich) (pH 7.2) for 10 min and then rinsed in PBS buffer three times (10 min each). The samples were then osmotically dehydrated through a graded water-ethanol series (35, 50, 70, 80, 95, and 100%, 20 min each step) and then lyophilized. Scaffolds were sputter-coated with gold and the morphology of the fibroblast cells were analyzed by SEM.

2.5.3. Apoptotic assay by acridine orange-ethidium bromide staining

To evaluate the presence of apoptotic cells and the possible effects of cytotoxicity of the CNF scaffolds the seeded BALB-3T3 cells were stained with a mixture of acridine orange (AO, Sigma-Aldrich) and ethidium bromide (EtBr, Sigma-Aldrich) at concentration of 100 μg.mL^{-1} in PBS for 20 s. Samples were observed and photographed with a Carl Zeiss fluorescence microscope equipped with epifluorescence optics (Axioskop 40®/Axioskop 40 FL®). The emitted fluorescence for AO was acquired at 500–560 nm, and for EtBr, the emission was acquired at 600–700 nm.

2.6. Statistical analysis

Data represent the mean ± standard deviation (SD) of at least four replications. Statistical significance was tested by one-way ANOVA and Tukey and p-values inferior to 0.05 were considered significant.

3. Results and discussion

3.1. Scaffold preparation and characterization

Figure 1 shows the CEL production from PPW. The method for the production of scaffolds starts with the treatment of PPW with NaOH at 80 °C to accelerate the delignification with recovery of the CEL fibers (Figure 1A). It can be assumed that in this step 90–95% of the hemicellulose and lignin are dissolved and degraded during this process. The deposited lignin confers a dark colour to the pulp and, after the

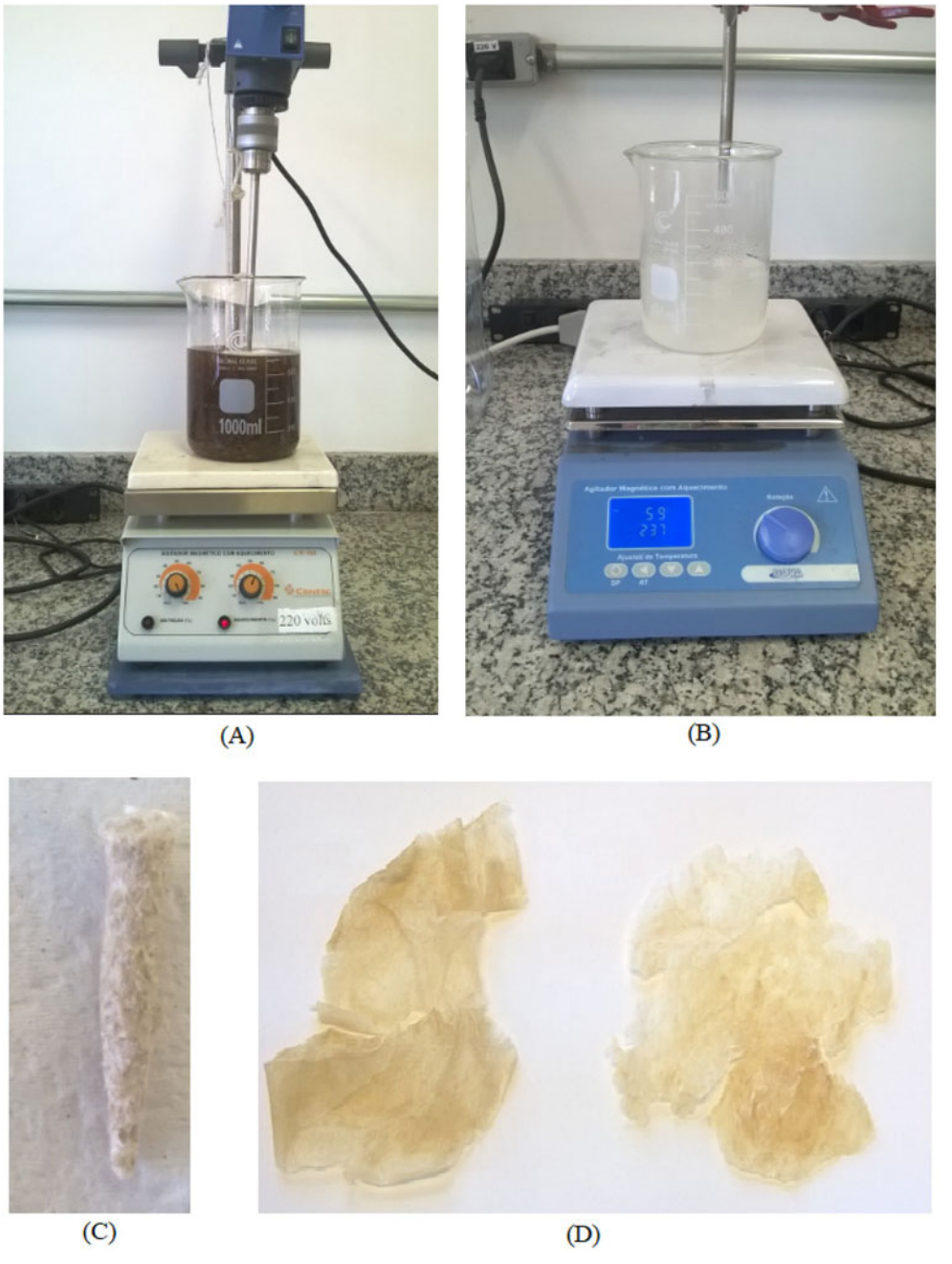

Figure 1. Stages of CEL extraction from PPW: potatoes peels during the stage of hemicellulose and lignin extraction (A), stage of bleaching through the use of hydrogen peroxide (B), aspect of the cellulose after sodium hydroxide process and H_2O_2 blenching (C), CEL films after blenching (D).

brown mass is thoroughly washed with deionized water, a bleaching was carried out with H_2O_2 (Figure 1B) for the removal of impurities and the remaining lignin. After bleaching the pulp attains a very clear colour (Figure 1C) providing the production of films (Figure 1D) suitable for use in electrospinning process.

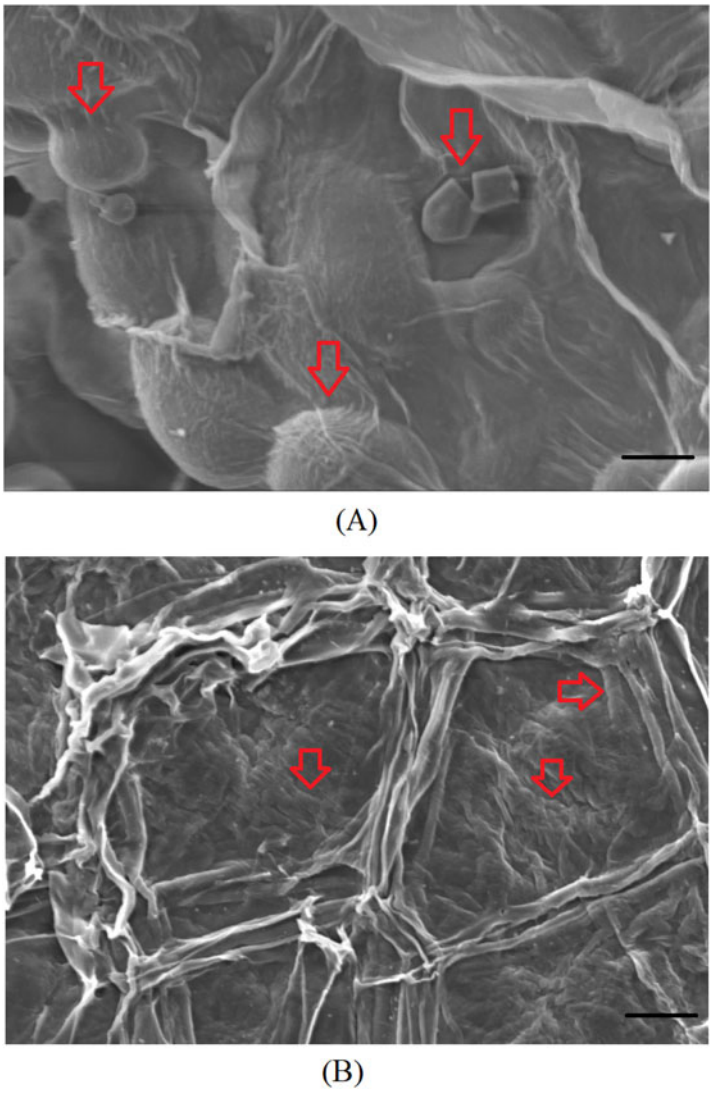

Figure 2. Scanning electron micrographs of PPW (A) and the extracted CEL (B). The arrows indicate the presence of starch granules before the delignification process (A) and delineated microfibrils after delignification process (B).The bars indicates 10 μm.

Figure 2 shows the scanning electron microscopy (SEM) to obtain qualitative information about the efficiency of the alkaline delignification process in the extraction of CEL from PPW. When examined by SEM PPW exhibit starch granules in spheres or polygonal shapes with size around 2–30 μm (Figure 2A) [38,39]. After the delignification it was observed that microfibrils were more clearly delineated indicating the higher lignin removal from the PPW. These observations are in good agreement with the results obtained from the cellulose SEM studies of other authors [40,41].

The ATR-FTIR spectra for the PPW and extracted CEL samples are shown in Figure 3A. Comparing the results, it is observed that PPW presents absorption bands related to three main peel components (cellulose, hemicellulose and lignin), while

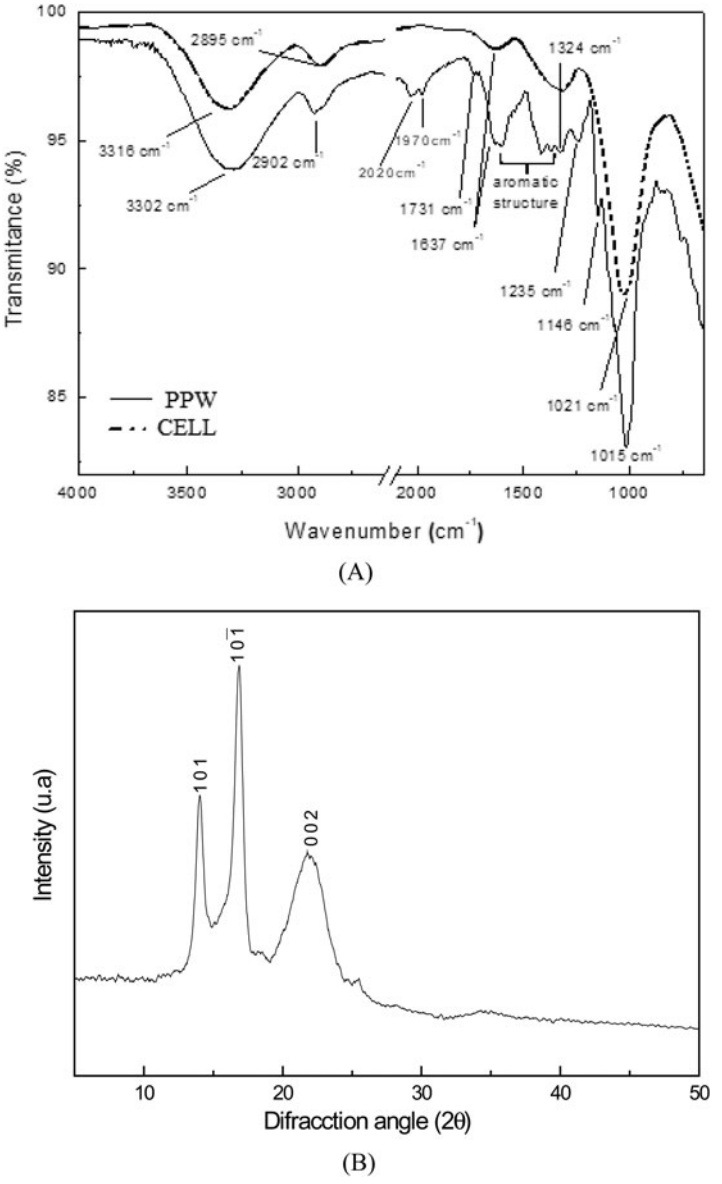

Figure 3. ATR-FTIR spectra (A) and XRD (B) of purified CEL from PPW.

extracted CEL demonstrates more bands that confirm the presence of cellulose. Both spectra present hydrogen bond stretching in the hydroxyl at 3300–3400 cm^{-1} [42] and the aliphatic saturated C-H stretching vibration at 2800–2900 cm^{-1} [12]. The unique fingerprint region for cellulose (800–1500 cm^{-1}) is also verified for PPW and extracted CEL, indicating that regardless of alkali or acid treatment, the cellulose chemical structure stays the same [32].

In the PPW spectrum, the absorption band at 1637 cm^{-1} is characteristic of the hemicelluloses and lignin ester groups vibration [43] and the range between 1600–1400 cm^{-1} is related to C = C vibration in lignin aromatic rings [12].

Furthermore, a band at 1235 cm^{-1} (C-O-C stretching), related to ether and ester bonds and responsible for the strong association between hemicellulose and lignin in the cell wall [44,45], which was only seen with PPW. Thus, these results confirm that treatment with NaOH and H_2O_2 was effective in removing hemicellulose and lignin.

Plots of X ray diffraction intensities from CEL extracted from PPW is shown in Figure 3B. Diffraction peaks at $2\theta = 14^\circ$ (101), 16.8° ($10\bar{1}$) and 22° (002) (Figure 3B) confirmed the characteristic structure of cellulose type I [32,46] and demonstrates that the crystalline structure of the native cellulose in potatoes peels remained unchanged after the alkaline extraction and blenching with H_2O_2. The relative crystallinity calculated in according to Segal method was 70.8%.

The morphology of the electrospun CNF was studied by SEM and the results are shown in Figure 4A and B. From Figure 4A and B can be noted that the nanofibers obtained from the CEL-Cuen solution are of poor quality with formation of bead, bending and flat fibrous structures. It is possible that the viscoelasticity of the Cuen-CEL solution, charge density in the jet, and the surface tension of the solution leading to some instability in the electrical forces responsible for the formation of the Taylor cone thus forming nanofibers of poor quality [47–51]. To overcome the issue of bead formation and flat fibrous structures, HPGL ($M_w = 4$ kDa) was added to the CEL-Cuen solution to a slight improvement in conductivity due to the existence of polar groups in the HPGL molecule. Figure 4C shows SEM images of electrospun CNF obtained from solutions containing 4 wt % HPGL. As can be seen (Figure 4C) a significant improvement in the fibber morphology upon addition of HPGL with a considerable reduction in bead-density was attained. A bimodal distribution of CNF was observed with average diameters around 100 nm and 700 nm (Figure 4E).

3.2. Biocompatibility of BALB-3T3 cell with CNF scaffolds

The electrospun scaffolds are attractive for tissue engineering because of their inherent advantages of high surface area for cell attachment, controlled porous architecture, and a 3-D microenvironment for cell-cell contact that mimicking the filamentary structure of the extracellular matrix (ECM) [49,50]. Nowadays, electrospinning is an important method for scaffolds preparation with a wide spectrum of properties (chemical, physical and mechanical) [52,53]. The implanted electrospun scaffold should act as temporary substitute of the native extracellular matrix, enabling the ingrowth of a new tissue by attracting cells from surrounding and providing suitable physiological conditions for cellular proliferation [54].

Figure 5A and B demonstrates SEM morphologies of fibroblast adhesion onto CNF scaffolds. SEM micrographs data demonstrate that BALB3-T3 cells efficiently attached and spread to the CNF scaffolds in the first 24 h of cultivation in DMEM medium. Fibroblasts were grown on CNF scaffolds as well and the formation of a cell layer type fibroblast-like adhering firmly to CNF scaffolds was observed (Figure 5A and B).

Fluorescence AO/EtBr images and phase contrast images were taken to see the attachment of BALB-3T3 fibroblast cells over the CNF scaffold (Figure 6).

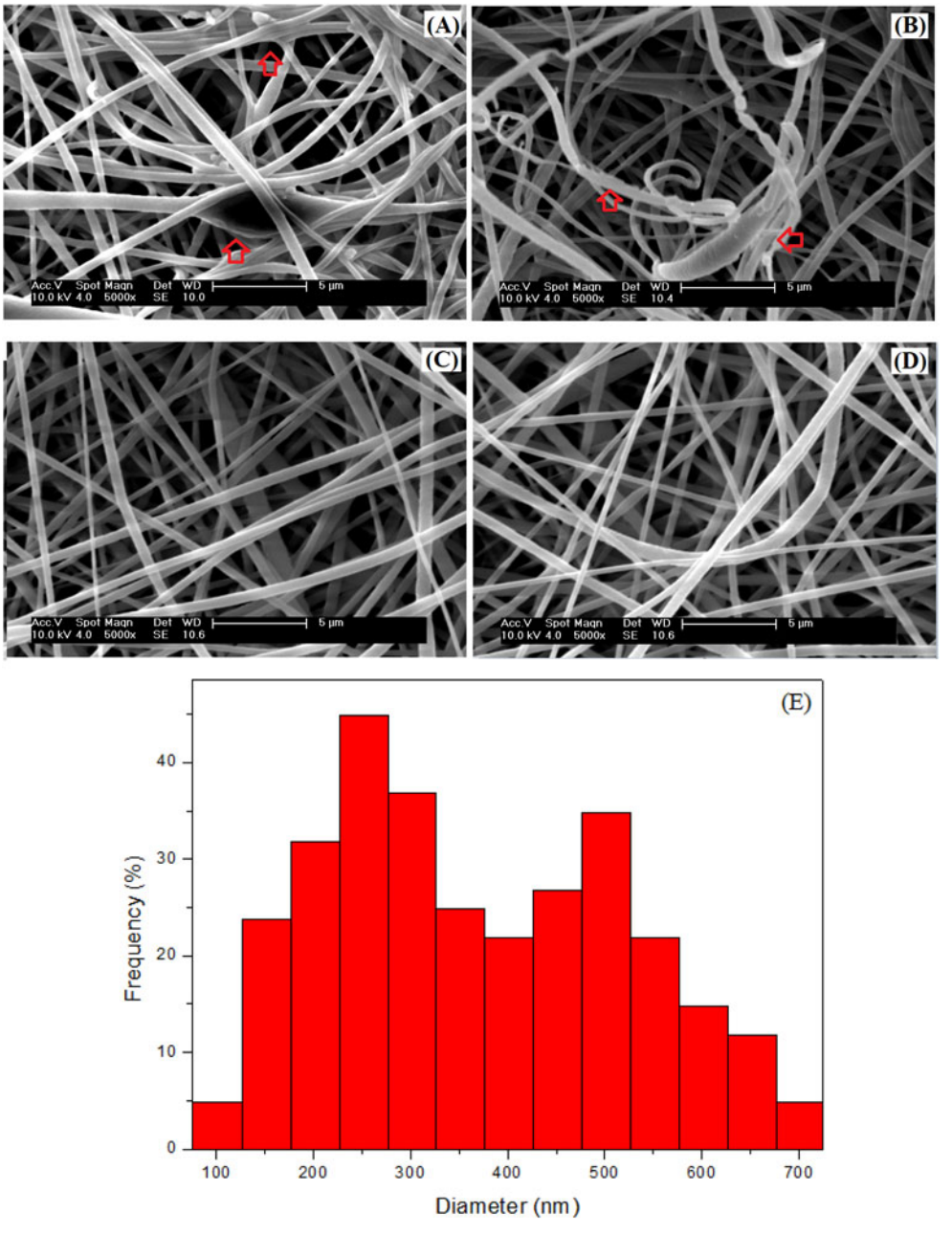

Figure 4. SEM images of electrospun CNF scaffolds produced from solutions of 10 wt % CEL-Cuen both without (A, B) and with addition of HPGL nonionic surfactant (C, D). The diameter distribution of CNF is shown in (E). Arrows indicates the fiber defects. The bars indicates 5 μm.

Additionally, these tests helped to know whether there was any change in the morphology of cells due to contact with the CNF scaffold and makes it possible to evaluate whether CNF scaffolds induced morphological alterations that could be attributed to an apoptotic/necrotic cellular mechanism [55,56]. Fluorescence microscopy after AO/EtBr staining allows visualizing apoptosis related changes in BALB-3T3 cells and their

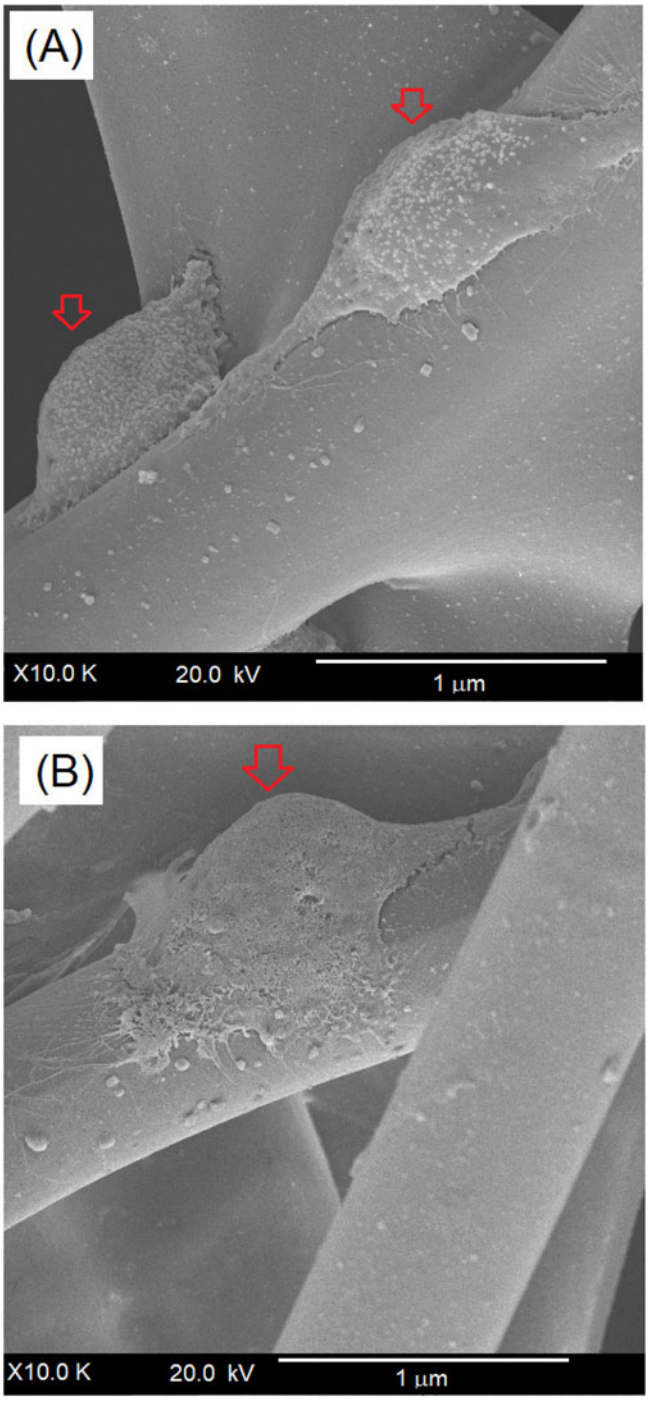

Figure 5. Scanning electron micrographs of BALB-3T3 cells adhered on CNF scaffolds after 24 hours of culture. Arrows indicates de BALB-3T3 cells adhered on CNF structure. Scale bar indicates 1 μm. It was observed that the fibroblasts adhere in the fibers of greater diameter which suggests the existence of a critical size for the beginning of adhesion.

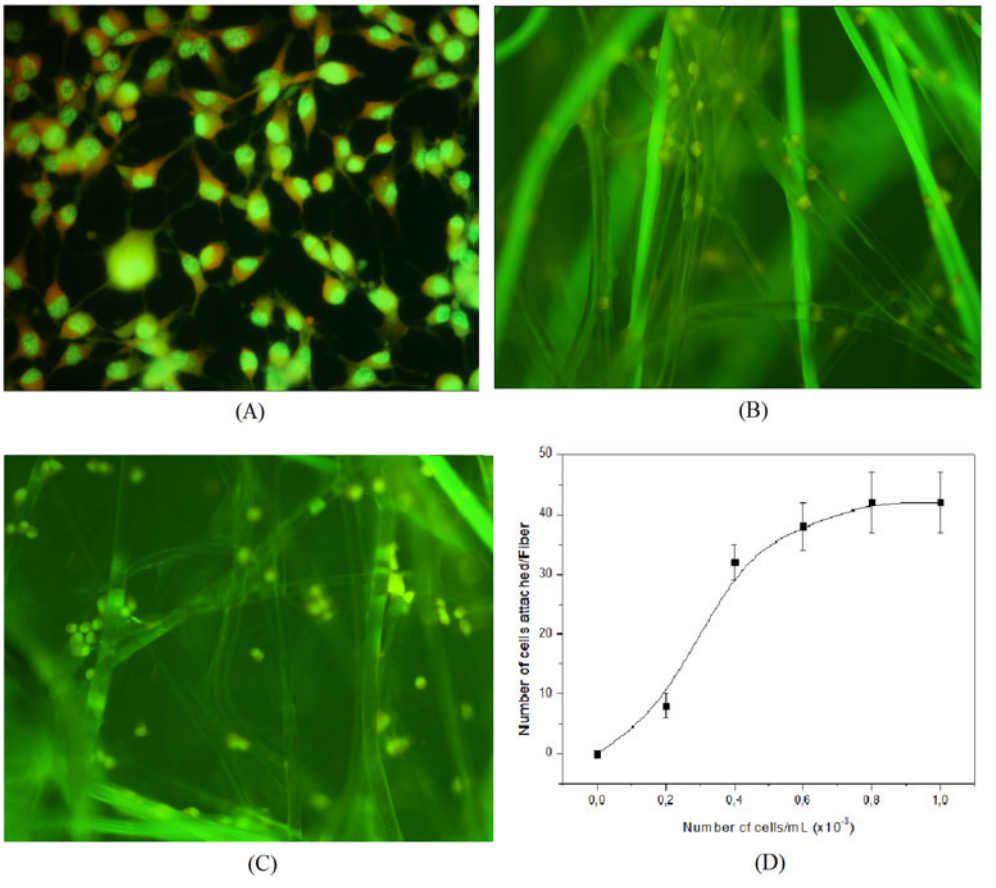

Figure 6. Representative fluorescence microscopy images (40X magnification) show AO/EtBr stained BALB-3T3 seeded cells on control (A) and CNF scaffolds (B, C). In (D) are shown the relationship between cell seeding concentration and the number of attached cells on the fibers. The averages of the cells number presenting the numbers of cells attached on the CNF among different concentrations of cells in the medium (numbers/mL). The experiments were performed independently five times. Error bars (D) show the standard deviation.

nuclei in order to verify cell viability. Live cells appear green (with acridine orange), while apoptotic cells appear orange (with ethidium bromide). Initially, BALB-3T3 fibroblast cells adhesion and spreading over the CNF electrospun scaffold would be considered as essential step for cell growth required for wound healing and restoration of the tissues. All images (Figure 6B and C) clearly proved that normal morphology of spindle-like shapes of live BALB-3T3 cells was maintained even after 3 days for CNF scaffold. Fluorescence images also proved that BALB-3T3 cells adhering through CNF nanofibers are viable, represented by the lysosomes stained by AO and suggest the absence of dead cells since the presence of EtBr positive cells have not been observed.

The degree of BALB-3T3 cell adhesion onto CNF scaffolds was quantified from fluorescence microscopy by measuring the number of cells that adhered onto each fibber as a function of the initial cell seeding density (Figure 6D). There was a

sigmoidal trend between the number of cells seeded and the number of cells that were adhered on the CNF nanofiber scaffolds.

4. Conclusions

CEL was extracted and purified from PPW, a biomass resource known as agricultural waste. ATR-FTIR and XRD of the extracted CEL confirmed their quality and purity. The electrospinning technique provides an efficient approach to fabricating CNF scaffolds with diameters in the nanometer range with bimodal size distribution. In the present study, CNF scaffold supported the adhesion and growth of BALB-3T3 cells. The results obtained from the fluorescence and scanning electron microscopy indicates that BALB-3T3 cells were growing onto electrospun CNF scaffold. However, despite the positive in vitro results, in vivo and clinical trials should be performed to confirm whether the fibroblast adhesion and proliferation properties of CNF may lead to a better formation of a collagenous connective tissue in the clinical setting. In the light of the low cost of PPW, the results of in vitro assays suggest that CNF extracted from PPW has a significant potential to be a suitable scaffold tissue engineering applications.

Disclosure statement

No potential conflict of interest was reported by the authors.

Funding

This study was funded by the National Council for Scientific and Technological Development (CNPq) and Coordination of Improvement of Higher Level Personnel (Capes).

ORCID

Maria Elena Leyva González http://orcid.org/0000-0003-0673-5713
Alvaro Antonio Alencar de Queiroz http://orcid.org/0000-0002-1769-7022

References

[1] Williams CK, Hillmyer MA. Polymers from renewable resources: a perspective for a special issue of polymer reviews. Polymer Revs. 2008;48:1–10.
[2] Gandini A. Polymers from renewable resources: a Challenge for the future of macromolecular materials. Macromolecules. 2008;41:9491–9504.
[3] Sahu P, Sarkar P, Bhowmick AK. Design of a molecular architecture via a green route for an improved silica reinforced nanocomposite using bioresources. ACS Sustainable Chem Eng. 2018;6:6599–6611.
[4] Valerio O, Misra M, Mohanty AK. Poly(glycerol-co-diacids) polyesters: from glycerol biorefinery to sustainable engineering applications, a review. ACS Sustainable Chem Eng. 2018;6:5681–5693.
[5] Van de Fliert E, Braun AR. Conceptualizing integrative, farmer participatory research for sustainable agriculture: from opportunities to impact. Agric Human Values. 2002; 19:25–38.

[6] Rodrigues GS, Campanhola C, Kitamura PC. An environmental impact assessment system for agricultural R&D. Environ Impact Assess Rev. 2003;23:219–244.
[7] Chen G-Q, Patel MK. Plastics derived from biological sources: present and future: a technical and environmental review. Chem Rev. 2012;112:2082–2099.
[8] Cateto CA, Barreiro MF, Rodrigues AE. Monitoring of lignin-based polyurethane synthesis by FTIR-ATR. Ind Crops Prod. 2008;27:168–174.
[9] Briassoulis D, Babou E, Hiskakis M, et al. Review, mapping and analysis of the agricultural plastic waste generation and consolidation in Europe. Waste Manag Res. 2013;31:1262–1278.
[10] Davis G, Song JH. Biodegradable packaging based on raw materials from crops and their impact on waste management. Ind Crops Prod. 2006;23:147–161.
[11] Halterman D, Guenthner J, Collinge S, et al. Biotech potatoes in the 21st century: 20 years since the first biotech potato. Am J Potato Res. 2016;93:1–20.
[12] Liang S, McDonald AG. Chemical and thermal characterization of potato peel waste and its fermentation residue as potential resources for biofuel and bioproducts production. J Agric Food Chem. 2014;62:8421–8429.
[13] Smerilli M. Valorization of potato-processing residues for the production of lactic acid. ChemBiochemEngQ. 2016;30:255–263.
[14] Kang HJ, Min SC. Potato peel-based biopolymer film development using high-pressure homogenization, irradiation, and ultrasound. LWT - Food Sci Technol. 2010;43:903–909.
[15] Lappalainen K, Kärkkäinen J, Joensuu P, et al. Modification of potato peel waste with base hydrolysis and subsequent cationization. Carbohydr Polym. 2015;132:97–103.
[16] Kumar VB, Pulidindi IN, Gedanken A. Glucose production from potato peel waste under microwave irradiation. J Mol Catal A Chem. 2016;417:163–167.
[17] Haider A, Haider S, Kang I-K. A comprehensive review summarizing the effect of electrospinning parameters and potential applications of nanofibers in biomedical and biotechnology. Arab J Chem. 2018;11:1165–1188.
[18] Frey MW. Electrospinning cellulose and cellulose derivatives. Polym Rev. 2008;48:378–391.
[19] Chahal S, Hussain FSJ, Kumar A, et al. Fabrication, characterization and in vitro biocompatibility of electrospun hydroxyethyl cellulose/poly (vinyl) alcohol nanofibrous composite biomaterial for bone tissue engineering. Chem Eng Sci. 2016;144:17–29.
[20] Naseri N, Poirier JM, Girandon L, et al. 3-Dimensional porous nanocomposite scaffolds based on cellulose nanofibers for cartilage tissue engineering: Tailoring of porosity and mechanical performance. RSC Adv. 2016;6:5999–6007.
[21] Naseri N, Mathew AP, Girandon L, et al. Porous electrospun nanocomposite mats based on chitosan–cellulose nanocrystals for wound dressing: effect of surface characteristics of nanocrystals. Cellulose. 2015;22:521–534.
[22] Čolić M, Mihajlović D, Mathew A, et al. Cytocompatibility and immunomodulatory properties of wood based nanofibrillated cellulose. Cellulose. 2015;22:763–778.
[23] Bodin A, Ahrenstedt L, Fink H, et al. Modification of nanocellulose with a xyloglucan-RGD conjugate enhances adhesion and proliferation of endothelial cells: Implications for tissue engineering. Biomacromolecules. 2007;8:3697–3704.
[24] Entcheva E, Bien H, Yin L, et al. Functional cardiac cell constructs on cellulose-based scaffolding. Biomaterials. 2004;25:5753–5762.
[25] Müller FA, Müller L, Hofmann I, et al. Cellulose-based scaffold materials for cartilage tissue engineering. Biomaterials. 2006;27:3955–3963.
[26] Vatankhah E, Prabhakaran MP, Jin G, et al. Development of nanofibrous cellulose acetate/gelatin skin substitutes for variety wound treatment applications. J Biomater Appl. 2014;28:909–921.
[27] Löbmann K, Svagan AJ. Cellulose nanofibers as excipient for the delivery of poorly soluble drugs. Int J Pharm. 2017;533:285–297.

[28] Zang S, Zhang R, Chen H, et al. Investigation on artificial blood vessels prepared from bacterial cellulose. Mater Sci Eng C. 2015;46:111–117.
[29] Mohamad R, Nayeri MD, Rahman HS, et al. Potential use of plant fibres and their composites for biomedical applications. BioResources. 2014;9:5688–5706.
[30] Singh BN, Panda NN, Mund R, et al. Carboxymethyl cellulose enables silk fibroin nanofibrous scaffold with enhanced biomimetic potential for bone tissue engineering application. Carbohydr Polym. 2016;151:335–347.
[31] Gaihre B, Jayasuriya AC. Fabrication and characterization of carboxymethyl cellulose novel microparticles for bone tissue engineering. Mater Sci Eng C. 2016;69:733–743.
[32] Chen D, Lawton D, Thompson MR, et al. Biocomposites reinforced with cellulose nanocrystals from potato peel waste. Carbohydr Polym. 2012;90:709–716.
[33] Wu D. Recycle technology for potato peel waste processing: a review. Procedia Environ Sci. 2016;31:103–107.
[34] Saalwächter K, Burchard W, Klüfers P, et al. Cellulose solutions in water containing metal complexes. Macromolecules. 2000;33:4094–4107.
[35] Fernandes EGR, De Queiroz AA. A bioconjugated polyglycerol dendrimer with glucose sensing properties. J Mater Sci: Mater Med. 2009;20:473–479.
[36] Yue D, Qian X. Isolation and rheological characterization of cellulose nanofibrils (CNFs) from coir fibers in comparison to wood and cotton. Polymers (Basel). 2018;10: 320–312.
[37] Ziabari M, Mottaghitalab V, McGovern ST, et al. A new image analysis based method for measuring electrospun nanofiber diameter. Nanoscale Res Lett. 2007;2:597–600.
[38] Pérez S, Baldwin PM, Gallant DJ. Structural features of starch granules II. In Starch: chemistry and technology. 3rd ed. New York (NY): Elsevier Inc.; 2009. p. 193–236.
[39] Huang J, Hess WM, Weber DJ, et al. Scanning electron microscopy: tissue characteristics and starch granule variations of potatoes after microwave and conductive heating. Food Struct. 1990;9:113–122.
[40] Saka S. Evaluation of the quantitative assay of lignin distribution by SEM-EDXA-technique. Wood Sci Technol. 1982;16:1–18.
[41] Fromm J, Rockel B, Lautner S, et al. Lignin distribution in wood cell walls determined by TEM and backscattered SEM techniques. J Struct Biol. 2003;143:77–84.
[42] Kumar A, Singh Negi Y, Choudhary V, et al. Characterization of cellulose nanocrystals produced by acid-hydrolysis from sugarcane bagasse as agro-waste. J Mater Phys Chem. 2014;2:1–8.
[43] Sun XF, Xu F, Sun RC, et al. Characteristics of degraded cellulose obtained from steam-exploded wheat straw. Carbohydr Res. 2005;340:97–106.
[44] Atsushi K, Azuma J. I, Tetsuo K. Lignin-carbohydrate complexes and phenolic acids in bagasse. Holzforschung. 1984;38:141–149.
[45] Yang H, Yan R, Chen H, et al. Characteristics of hemicellulose, cellulose and lignin pyrolysis. Fuel. 2007;86:1781–1788.
[46] Ford ENJ, Mendon SK, Thames SF, et al. X-ray diffraction of cotton treated with neutralized vegetable oil-based macromolecular crosslinkers. J Eng Fiber Fabr. 2010;5: 10–20.
[47] Kim CW, Kim DS, Kang SY, et al. Structural studies of electrospun cellulose nanofibers. Polymer (Guildf). 2006;47:5097–5107.
[48] Ohkawa K. Nanofibers of cellulose and its derivatives fabricated using direct electrospinning. Molecules. 2015;20:9139–9154.
[49] Khatri Z, Wei K, Kim BS, et al. Effect of deacetylation on wicking behavior of co-electrospun cellulose acetate/polyvinyl alcohol nanofibers blend. Carbohydr Polym. 2012;87: 2183–2188.
[50] Celebioglu A, Uyar T. Electrospun porous cellulose acetate fibers from volatile solvent mixture. Mater. Lett. 2011;65:2291–2294.
[51] Theron SA, Zussman E, Yarin AL. Experimental investigation of the governing parameters in the electrospinning of polymer solutions. Polymer (Guildf). 2004;45:2017–2030.

[52] Lannutti J, Reneker D, Ma T, et al. Electrospinning for tissue engineering scaffolds. Mater Sci Eng C. 2007;27:504–509.
[53] Sun B, Long YZ, Zhang HD, et al. Advances in three-dimensional nanofibrous macrostructures via electrospinning. Prog Polym Sci. 2014;39:862–890.
[54] O'Brien FJ. Biomaterials & scaffolds for tissue engineering. Mater Today. 2011;14:88–95.
[55] Gherghi IC, Girousi ST, Voulgaropoulos AN, et al. Study of interactions between DNA-ethidium bromide (EB) and DNA-acridine orange (AO), in solution, using hanging mercury drop electrode (HMDE). Talanta. 2003;61:103–112.
[56] Baskić D, Popović S, Ristić P, et al. Analysis of cycloheximide-induced apoptosis in human leukocytes: fluorescence microscopy using annexin V/propidium iodide versus acridin orange/ethidium bromide. Cell Biol Int. 2006;30:924–932.